Published in Finite Elements in Analysis and Design, 76: pp. 63-70.
DOI: 10.1016/j.finel.2013.08.002

Modelling facial expressions: a framework for simulating nonlinear soft tissue deformations using embedded 3-D muscles

Tim Wu[a], Alice P.-L. Hung[a], Peter Hunter[a], Kumar Mithraratne[a]

[a] Auckland Bioengineering Institute, The University of Auckland, Auckland, New Zealand

Human face can be seen as a soft tissue organ complex with a large investing network of musculature. Due to its complexity, most existing computational models approximate these muscular structures using simple geometries such as 1-D curves or primitive 3-D shapes. This paper presents a new approach to evaluate muscle contribution from anatomically accurate geometries while maintaining the computational complexity at a tractable level. In the proposed method, 3-D muscle structures are embedded inside a facial continuum (encompassing all superficial soft tissue structures), where mechanical contribution of muscles is evaluated independently and transferred to the facial computational domain through a finite element mapping procedure. Muscle forces are decomposed into an array of discrete point loads that are determined at the integration points of an appropriate quadrature scheme. As a result, muscle meshes can be constructed independent from the facial mesh giving two main advantages: (i) the muscle geometries can be refined independent of the facial computational domain, and (ii) it is not required for the computational domain to conform to complex topology of muscle structures.

Keywords: Facial biomechanics; Embedded muscles; Nonlinear elasticity; Anisotropy; Cubic Hermite elements; Mixed finite element method

1 Introduction

Generating facial expressions using anatomically accurate biomechanical models have many applications in entertainment, security and medicine. One important advantage of having a muscle-driven biomechanical face model is that it can produce realistic expressions while interacting with the environment [1]. In facial recognition, a biomechanical model allows detection of an input face with a different expression than available in the training database [2]. Human face models are also used in speech production simulations [3] and to evaluate both aesthetic and functional outcomes of a surgery [4,5]. In all of these, it is important for the numerical predictions of the soft tissue deformation to be reliable and accurate, especially in speech simulations and surgical planning.

Modelling the mechanics of a human face is a computationally challenging task. This is partly due to the fact that facial soft tissues often undergo large local rotations and

Published in Finite Elements in Analysis and Design, 76: pp. 63-70.
DOI: 10.1016/j.finel.2013.08.002

straining. Thus, nonlinear, finite deformation (large deformation) elasticity theory is required to model these deformations accurately. In addition, facial soft tissues, like many other biological tissues, are structurally complex [6,7], and exhibit nonlinear constitutive behaviour [8]. Analysing muscle contraction at the whole face level presents even more fascinating challenge as computer modellers must also consider the directional mechanical contribution of individual muscle fascicles that are part of a complex muscular network. Almost all early computational models of the human face treated muscular structures as series of line segments [9–11]. However, these linear 1-D models were incapable of recreating the paths of muscles with complex geometry. In addition, they often disregarded the heterogeneous and anisotropic mechanical response resulted from the embedded fibrous structures. Some of these issues have been addressed by more recent muscle models. For example, Gladilin et al. [12] proposed a virtual fibre model where muscle fibres were described as a vector field inside a 3-D ellipsoid. Similarly, Sifakis et al. [1] and Nazari et al. [13] used multiple 1-D spline and cable elements to approximate 3-D geometries. Another common approach is to model these muscles and other facial structures as discrete element regions. For example, Chabanas et al. [14] labelled certain elements inside the face mesh as muscle elements, where forces were applied on the nodes of these elements in direction of muscle fibres. Nevertheless, these techniques require extensive manipulation of the face mesh and often lacked anatomical accuracy.

This paper presents a new approach for modelling complex musculature inside the human face based on the theory of finite elasticity. The governing equations are numerically solved using the finite element method. In the proposed implementation, we treat facial tissues as incompressible and hyperelastic material. 3-D muscle structures are embedded inside a single face continuum through a finite element coordinate mapping procedure. In order to ensure anatomical accuracy, all finite element volume meshes (face continuum and individual muscles) were generated using the data derived from the visible human cryosection images [15].

A brief description pertinent to the theory of finite elasticity and finite element method is presented in the next section. This is followed by the details of constitutive relations of the facial tissues and muscle fibres adapted in our model and the formulation of the finite element model. Creation of anatomically accurate geometries of the model structures is outlined next. In the subsequent section, simulation results are presented. Finally a discussion highlighting strengths and weaknesses of the framework is provided.

Published in Finite Elements in Analysis and Design, 76: pp. 63-70.
DOI: 10.1016/j.finel.2013.08.002

2 Modelling principles

Finite elasticity theory with finite element implementation is a common mathematical approach for describing the principles of continuum mechanics applied to biological soft tissues. In contrast to linear elasticity, finite elasticity theory is able to accurately predict nonlinear kinematics of mechanically nonlinear materials that undergo large local rotations and large straining. For a comprehensive introduction to the nonlinear continuum mechanics, the reader is referred to [16]. This section provides a brief summary of the theory, which is fundamental to modelling the biomechanics of the human face.

In order to describe the large deformations of a body, we first need to consider the kinematic relationship between the body in the reference (undeformed) configuration, described by $\mathbf{X}=(X_1, X_2, X_3)$ and the current (deformed) configuration, described by $\mathbf{x}=(x_1, x_2, x_3)$, in the spatial Cartesian coordinate system. Here, $\mathbf{x}$ is a continuous, differentiable and a single-valued function of $\mathbf{X}$: $\mathbf{x}=\mathbf{X}+\mathbf{u}(\mathbf{X})$, with $\mathbf{u}$ being the displacement from the reference to the current configuration. The deformation gradient tensor $\mathbf{F}=\partial\mathbf{x}/\partial\mathbf{X}$ quantifies this spatial transformation. According to the principle of virtual work, the external virtual work (δW_{ext}) due to an arbitrary virtual displacement ($\delta\mathbf{u}$), is equal to the internal virtual work (δW_{int}) stored in the body: $\delta W_{ext}=\delta W_{int}$.

For a static equilibrium, the virtual work statements can be described as

$$\begin{aligned}\delta W_{int} &= \int_v \boldsymbol{\sigma} : \left[\frac{\partial \delta \mathbf{u}}{\partial \mathbf{x}}\right] dv \\ \delta W_{ext} &= \int_v \mathbf{f}\cdot\delta\mathbf{u}\, dv + \int_s \mathbf{t}\cdot\delta\mathbf{u}\, ds\end{aligned} \tag{1}$$

Here, $\boldsymbol{\sigma}$ is the Cauchy stress tensor, $\mathbf{f}$ and $\mathbf{t}$ are the body force and boundary traction vectors in the current configuration, v and s are the current volume and surface area of the body respectively.

2.1 Finite element method

In order to solve equation 1, the finite element method (FEM) is used. In the FEM, all variables are approximated as piecewise polynomials controlled by a finite number of nodal parameters. Moreover, in the case of finite elasticity with incompressible

Published in Finite Elements in Analysis and Design, 76: pp. 63-70.
DOI: 10.1016/j.finel.2013.08.002

materials, mixed-FEM (displacement-pressure) implementation is required [17], Thus, the two dependent fields, displacement **u** and pressure *p* (a detailed description of *p* is given in section 3) are given by the following finite element interpolation scheme.

$$\begin{aligned} \mathbf{u} &= \sum_n \psi_n^{(u)}(\boldsymbol{\xi}) \cdot \mathbf{u}_n \\ p &= \sum_n \psi_n^{(p)}(\boldsymbol{\xi}) \cdot p_n \end{aligned} \tag{2}$$

Where $\mathbf{u}_n$ and p_n are nodal parameters of displacement and pressure fields respectively. $\psi_n^{(u)}$ and $\psi_n^{(p)}$ are associated basis functions and $\boldsymbol{\xi} = (\xi_1, \xi_2, \xi_3)$ are the normalised element coordinates. In order to better satisfy the physical conditions for realistic soft tissue deformations such as large bending and torsion, derivative continuous (C1-continuous) cubic Hermite basis functions are used to interpolate the displacement field [18]. Furthermore, to avoid ill-conditioning, basis functions for the pressure field are required to be at least one order of polynomial lower than that used for the geometric field [16]. In this study, the pressure field is interpolated using linear Lagrange basis functions.

3 Modelling approach

3.1 Constitutive relation of facial tissue

3.1.1. Adipose and connective tissues

The human face primarily consists of mechanically passive adipose and connective tissues. These materials are often approximated as isotropic and hyperelastic [4,13,19]. In this paper, we model facial tissues as incompressible Mooney–Rivlin solid whose constitutive properties can be expressed using a scalar strain energy density function as follows:

$$w = c_1(\bar{I}_1 - 3) + c_2(\bar{I}_2 - 3) - p(J - 1) \tag{3}$$

where c_1 and c_2 are the parameters relating to the elastic distortion of the material, $\bar{I}_1$ and $\bar{I}_2$ are the isochoric strain invariants derived from the isochoric deformation tensor [20]. The derivatives of w with respect to energetically conjugated strain give stress tensor:

Published in Finite Elements in Analysis and Design, 76: pp. 63-70.
DOI: 10.1016/j.finel.2013.08.002

$$\boldsymbol{\sigma}_{face} = 2\left(c_1\mathbf{B} + c_2\left(I_1\mathbf{B} - \mathbf{B}^2\right) - \left(\frac{1}{3}c_1\bar{I}_1 + \frac{2}{3}c_2\bar{I}_2\right)\mathbf{I}\right) - p \tag{4}$$

$\boldsymbol{\sigma}_{face}$ is the Cauchy stress tensor that is used to described the mechanical behaviour of the passive facial tissues. $\mathbf{B} = \mathbf{F}\mathbf{F}^{\mathrm{T}}$ is the Finger deformation tensor and $\mathbf{I}$ is the identity tensor. To enforce incompressibility during the deformation, a Lagrange multiplier constraint is used:

$$\delta W_{vol} = \int_v (J-1)\delta p dv = 0 \tag{5}$$

Where $J = \det \mathbf{F}$ is the Jacobian of transformation, and δp is the variation of the pressure variable. Using this constraint, p can be evaluated such that zero volume change ($J = 1$) is imposed over the integrated domain.

3.1.2 Constitutive relation of muscle fibres

Muscle fibres constitute the mechanically active component inside a muscle structure. The process of force generation inside a muscle fibre is well documented and can be described by the sliding filament model [21] and cross-bridge theory [22]. During contraction, the overlaps between the actin and myosin filaments increase, causing an overall shortening and thickening of the muscle fibre. In isometric contraction, the muscle fibre length is held constant, but produces increasing active force as the level of activation increases. The term tetanic tension depicts the active tension force produced from a muscle tetanised under isometric conditions.

It is well-known that the tetanic tension is a function of muscle fibre stretch ($\lambda = L/L_0$), where L_0 and L are the reference and current fibre lengths respectively; for skeletal muscles, tetanic tension curve has a local maximum at the experimentally determined optimal fibre stretch λ_{ofl}. In addition, it is also observed that muscle fibres developed passive restorative forces when elongated beyond the optimal fibre length [23]. The following piecewise functions given by Blemker et al. [24] reproduce the classical force-stretch relationship observed in human skeletal muscles:

Published in Finite Elements in Analysis and Design, 76: pp. 63-70.
DOI: 10.1016/j.finel.2013.08.002

$$f_{active}^{fibre}=\begin{cases}9(\lambda/\lambda_{ofl}-0.4)^2, & 0.4\lambda_{ofl}<\lambda\le 0.6\lambda_{ofl}\\ 1-4(1-\lambda/\lambda_{ofl})^2, & 0.6\lambda_{ofl}<\lambda<1.4\lambda_{ofl}\\ 9(\lambda/\lambda_{ofl}-1.6)^2, & 1.4\lambda_{ofl}\le\lambda<1.6\lambda_{ofl}\\ 0, & otherwise\end{cases}$$

$$f_{passive}^{fibre}=\begin{cases}P_1(e^{P_2(\lambda/\lambda_{ofl}-1)}-1), & \lambda_{ofl}<\lambda<\lambda^*\\ P_3\,\lambda/\lambda_{ofl}+P_4, & \lambda\ge\lambda^*\\ 0, & otherwise\end{cases} \tag{6}$$

In equation 6, f_{active}^{fibre} and $f_{passive}^{fibre}$ are the fibre force normalised to the tetanic (maximum active) tension at the optimal fibre stretch, λ^* represents the fibre stretch at which $f_{passive}^{fibre}$ becomes linear, P_3 and P_4 are defined such that $f_{passive}^{fibre}$ is C^0- and C^1-continuous at $\lambda=\lambda^*$.

To model the anisotropic response resulting from the preferential direction of muscle fibres, it is more convenient to introduce a structure-based mutually-orthogonal, curvilinear coordinate system $\boldsymbol{\upsilon}=(\upsilon_1,\upsilon_2,\upsilon_3)$. Here υ_1 axis is defined to align with the muscle fibre direction while υ_2 and υ_3 axes (which are orthogonal to each other) are in a plane normal to the υ_1 direction. Hence, the total stress due to active fibre contraction and passive stretch in the fibre direction is given by.

$$\boldsymbol{\sigma}_{muscle}=\left(\sigma_{active}^{fibre}+\sigma_{paasive}^{fibre}\right)\left[\frac{\partial\mathbf{x}}{\partial\upsilon_1}\right]\otimes\left[\frac{\partial\mathbf{x}}{\partial\upsilon_1}\right]^{\mathrm{T}} \tag{7}$$

Where σ_{active}^{fibre} and $\sigma_{paasive}^{fibre}$ are the active and passive muscle fibre stress defined along the fibre direction. These stresses can be evaluated from equation 6 for a given tetanic stress (σ_{max}):

$$\begin{aligned}\sigma_{active}^{fibre}&=a\left(\sigma_{max}f_{active}^{fibre}\lambda/\lambda_{ofl}\right)\\ \sigma_{passive}^{fibre}&=\sigma_{max}f_{passive}^{fibre}\lambda/\lambda_{ofl}\end{aligned} \tag{8}$$

In equation 8, $a\in[0,1]$ is the level of activation of the muscle fibre, it is assumed that the active fibre stress scales linearly with muscle activation. The ratio λ/λ_{ofl}

Published in Finite Elements in Analysis and Design, 76: pp. 63-70.
DOI: 10.1016/j.finel.2013.08.002

reflects the change in the tetanic stress due to the change of the sarcomere density from the deformation [24].

3.2 Formulation of finite element model from virtual work statement

In order to accurately model the mechanical contribution of muscle fibres inside the face continuum, fibre stresses need to be evaluated separately over their respective volume space. Hence the internal virtual work statement becomes:

$$\delta W_{int} = \int_{v_{face}} \boldsymbol{\sigma}_{face} : \left[\frac{\partial \delta \mathbf{u}}{\partial \mathbf{x}}\right] dv + \sum_{m} \left\{ \int_{v_{muscle}^{(m)}} \boldsymbol{\sigma}_{muscle}^{(m)} : \left[\frac{\partial \delta \mathbf{u}}{\partial \mathbf{x}}\right] dv \right\} \tag{9}$$

Using FEM, we can describe the muscle volume as a system of finite element coordinates $\boldsymbol{\eta}^{(m)} = \left(\eta_1^{(m)}, \eta_2^{(m)}, \eta_3^{(m)}\right)$. Since the space occupied by muscle fibres are contained inside the face continuum: $v_{muscle} \in v_{face}$, a unique mapping between the face continuum and each muscle structure can be determined, such that $\boldsymbol{\xi}^{(m)} = \left(\xi_1^{(m)}, \xi_2^{(m)}, \xi_3^{(m)}\right)$ corresponds to $\boldsymbol{\eta}^{(m)}$ but defined in the finite element coordinate system of the face mesh. Accordingly, we can map each and every material point in the muscle volume to the face continuum and vice versa. This enables transferring muscle fibre induced stresses to the facial computational domain:

$$\delta W_{int} = \delta \mathbf{u} \left\{ \begin{array}{l} \iiint_{v_{face}} \left[\frac{\partial \Psi(\boldsymbol{\xi})}{\partial \mathbf{x}}\right] \boldsymbol{\sigma}_{face} g^{(\xi)} d\xi_1 d\xi_2 d\xi_3 \\ + \sum_{m} \left(\iiint_{v_{muscle}^{(m)}} \left[\frac{\partial \Psi(\boldsymbol{\xi}^{(m)})}{\partial \mathbf{x}}\right] \boldsymbol{\sigma}_{muscle}^{(m)} g^{(\eta)} d\eta_1 d\eta_2 d\eta_3 \right) \end{array} \right\} \tag{10}$$

Equation 10 presents the finite element formulation of the internal virtual work statement used in this study. In the equation $g^{(\xi)}$ and $g^{(\eta)}$ are the Jacobian of coordinate transformations from the finite element coordinate systems to the spatial Cartesian coordinate system:

$$\begin{aligned} g^{(\xi)} &= \det\left[\frac{\partial \mathbf{x}}{\partial \boldsymbol{\xi}}\right] \\ g^{(\eta)} &= \det\left[\frac{\partial \mathbf{x}}{\partial \boldsymbol{\eta}}\right] \end{aligned} \tag{11}$$

Published in Finite Elements in Analysis and Design, 76: pp. 63-70.
DOI: 10.1016/j.finel.2013.08.002

Notice that in the internal virtual work statement, muscle stresses are evaluated over the muscle domain, independent to the face continuum. This allows an accurate depiction of the muscle mechanics irrespective to the face mesh discretisation. The integrations can be evaluated using Gaussian quadrature or other appropriate numerical integration method. Essentially, the integration points from the muscle meshes are mapped to the face mesh as discrete point loads, hence the extra computation lies in evaluating mechanics at these additional integration points for muscle contributions, but there are no additional degrees of freedom to the problem.

3.3 Muscle fibres architecture

The fibres in some skeletal muscles are arranged at an oblique angle to the muscle length, such as the in the case of convergent and pennate muscles [25]. In order to address this issue, we use three Eulerian angles to perform three sequential rotations on the original reference material coordinate system (see section 3.1.1). Furthermore, the Euler angles are prescribed at nodes and treated as a continuous finite element field which is interpolated using linear Lagrange basis functions. See [26] for details. Figure 1 shows the dependence of varying muscle fibre orientation on the deformation of a rectangular beam of soft tissue. Due to the orientation of the fibres, the deformation varies from bending to torsional distortion. Notice that the mesh element density of the muscle mesh is independent to that of the beam mesh, this is made possible due to the fact that we handle the numerical integration on the muscle and beam domains separately.

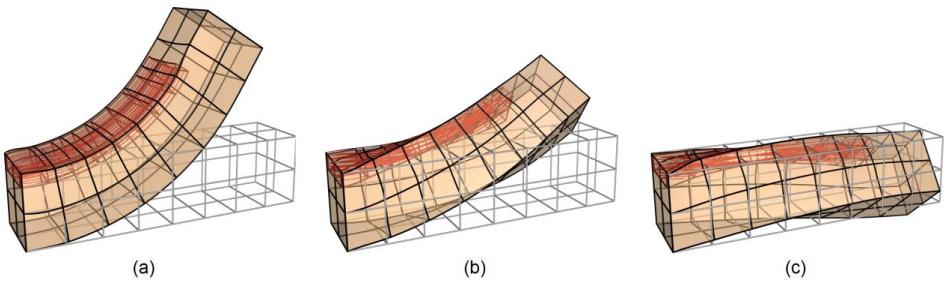

Figure 1 Deformation of a rectangular beam as a result of activation of a muscle slab embedded inside the beam. Showing muscle fibre angles of (a) 0°, (b) 36° and (c) 60° from η_1, which is the finite element axis of the muscle mesh along the length of the muscle.

Published in Finite Elements in Analysis and Design, 76: pp. 63-70.
DOI: 10.1016/j.finel.2013.08.002

4 Geometric models

The main mesh representing the facial continuum is a FE discretisation of the superficial fascia (SF) of the face [27], located between the external skin surface and the deep fascia. The superficial fascial layer is extracted from the Visible Human (VH) cryosection images [15]. Anatomically, the SF can be considered as superimposition of three distinct layers of structures [7], namely (from the external to internal layer), the dermis, subcutaneous tissues and the superficial musculoaponeurotic system (SMAS). An ultrasound study by Wu et al. [28] have revealed that these structures are kinematically coupled, hence a single continuous mesh is sufficient to model the deformation of the SF. The mesh is discretised into 560 hexahedral elements containing 1180 nodes (28320 geometric degrees of freedom with cubic Hermite interpolation). In order to reduce the number of degrees of freedom in our simulations, it is assumed the anatomy and the deformation is planar symmetric in the mid-sagittal plane (Figure 2).

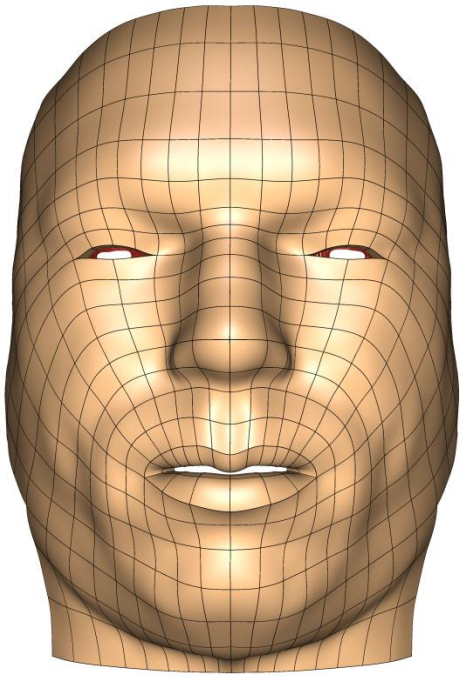

Figure 2 cubic-Hermite volume mesh of the Visible Human face created from the cryosection images

Published in Finite Elements in Analysis and Design, 76: pp. 63-70.
DOI: 10.1016/j.finel.2013.08.002

4.1 Facial muscles

15 pairs of facial muscles (Table 1) were considered in this study. Their respective mesh geometries were generated using the procedures documented in [29]. Platysma muscles were not included as their origins are at the clavicles, outside the coverage of the SF volume mesh. In addition, several other smaller muscles were also neglected. Figure 3 shows the position, geometry and the fibre orientation of all muscles that were included in the computational model. Close-up views of the zygomaticus major (parallel), orbicularis oris (circular) and buccinators (convergent) muscles are illustrated in Figure 4.

Table 1 Facial muscle names and abbreviation used in the simulation

Muscle name	Abbreviation
Buccinator	BUC
Corrugator supercilii	COR
Depressor anguli oris	DAO
Depressor labii inferioris	DLI
Frontalis	FRO
Levator anguli oris	LAO
Levator labii superioris	LLS
Levator labii superioris alaeque nasi	LLSAN
Mentalis	MEN
Orbicularis oris	OOR
Orbital orbicularis oculi	OOC
Palpebral orbicularis oculi	POC
Risorius	RIS
Zygomaticus major	ZMA
Zygomaticus minor	ZMI

Published in Finite Elements in Analysis and Design, 76: pp. 63-70.
DOI: 10.1016/j.finel.2013.08.002

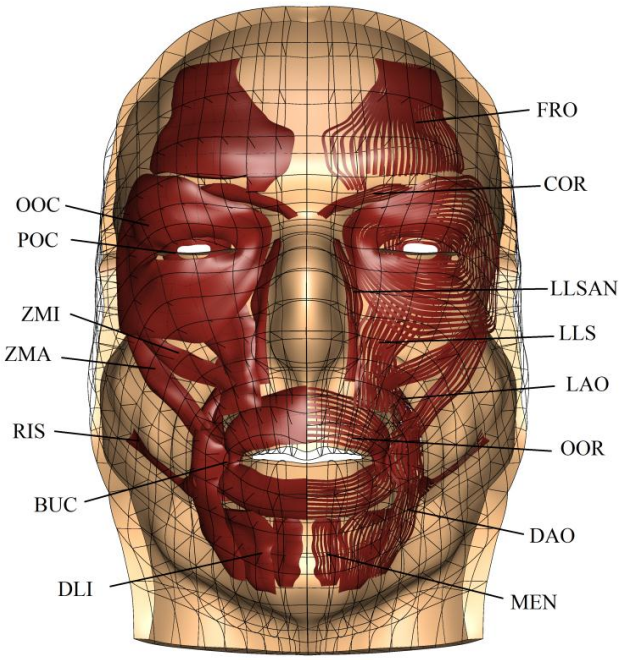

Figure 3 Location and geometry of the 15 facial muscles created from the cryosection images

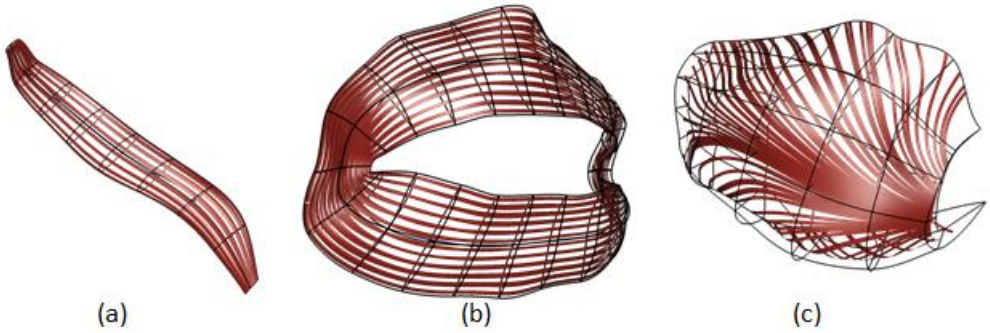

Figure 4 Muscle fibre orientations of (a) zygomaticus major, (b) orbicularis oris and (c) buccinators muscles.

4.2 Simulation conditions

Underneath the SF is the deep fascia (DF) consisting of deep masticatory muscles, salivary glands and fat pads. In some regions of the face, the SF is in direct contact with the mandible and maxilla. Consequently, a surface corresponding to the deep contact plane is required to simulate the physical contact conditions. Since soft tissues underneath the SF have less contribution to the formation of facial gestures, they are regarded as non-mobile rigid bodies in our current implementation. Two types of

Published in Finite Elements in Analysis and Design, 76: pp. 63-70.
DOI: 10.1016/j.finel.2013.08.002

contact are considered here. At the perioral region, collision detections are implemented between the SF and bones, as well as between the upper and lower lips. At the SF and DF interface, sliding interaction prevents the SF from detaching from the deep soft tissues. Both of these contact conditions assume zero friction.

Facial retaining ligaments [30] and muscles attachment points are included in our mechanical model as nodal boundary conditions. These constraints prevent excessive movement of the SF and provide integrity to the overall structure. Table 2 shows the material parameters (as described in section 3.1) used in the simulation. The effect of gravity is not considered.

Table 2 Constitutive model constants

Passive facial tissues constants	**Muscle fibre constants**
c_1 = 0.5kPa	σ_{max} = 300kPa
c_2 = 0.2kPa	λ^* = 1.4 (dimensionless)
	λ_{ofl} = 1 (dimensionless)
	P_1 = 0.005 (dimensionless)
	P_2 = 6.6 (dimensionless)

5 Facial expression simulations

This section demonstrates the numerical simulations of various facial expressions by activating relevant facial muscles using the proposed method. The results are consistent with other numerically studies [1, 4, 13] as well as descriptions reported in anatomical literature [25].

Orbicular oris muscle is a sphincter muscle that encircles the mouth. When activated, the muscle closes the mouth and puckers the lips (figure 5a). A smiling expression, can be generated by the coordinated contraction of four facial muscles (zyogmaticus major, zygomaticus minor, risorius and levator labii superioris muscles), which draws the angles of the mouth superiorly and posteriorly (Figure 5b). On the other hand, frowning expression is modelled by activating risorius, depressor labii inferioris, mentalis and corrugator muscles (Figure 5c).

Published in Finite Elements in Analysis and Design, 76: pp. 63-70.
DOI: 10.1016/j.finel.2013.08.002

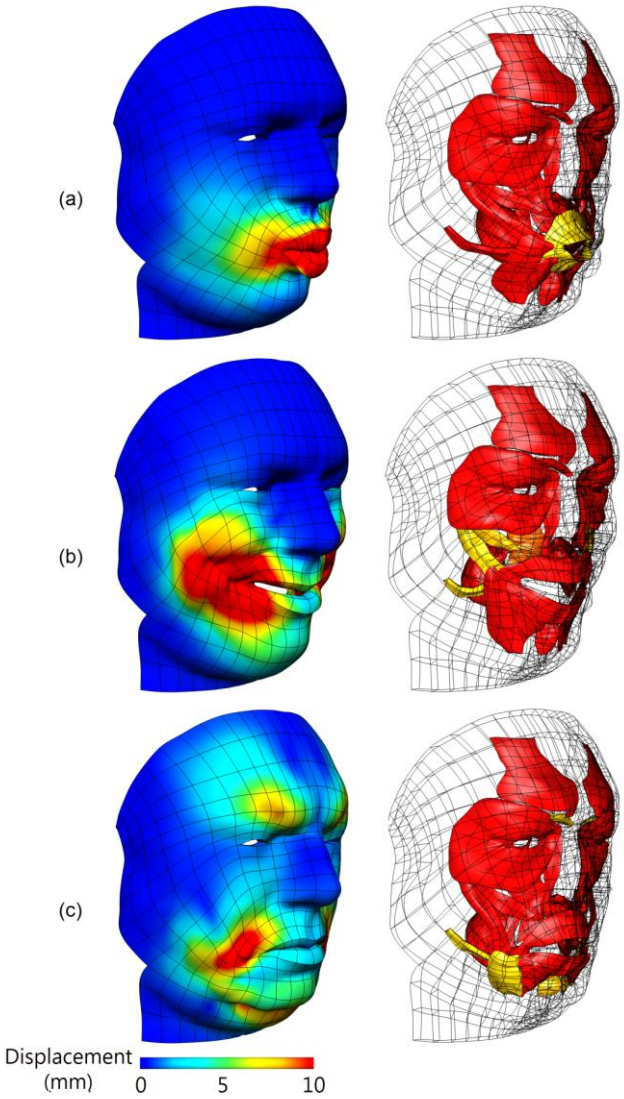

Figure 5 Simulations of (a) lips puckering, (b) smiling and (c) frowning by activating appropriate muscles.

6 Discussion and conclusion

The main objective of this work is to introduce a finite element framework for embedding complex, 3-D musculature for simulating and analysing mechanical deformation of the facial tissues due to muscle activation.

In comparison to models with 1-D muscles, 3-D muscle geometries have the ability to represent the curved path and shape of muscles with complex topology more accurately. In addition, the moment arms of each individual fascicles can also be more accurately reproduced, resulting in a better depiction of the muscle forces acting on

Published in Finite Elements in Analysis and Design, 76: pp. 63-70.
DOI: 10.1016/j.finel.2013.08.002

the bone [31]. Moreover, the use of realistic muscle geometry eliminates the need to assign heuristic parameters such as the number of virtual fibre bundles per muscle or the estimated physiological cross sectional area (PCSA) of the muscle geometry. Another advantage of our proposed framework is the independency between the muscle mesh and the discretisation of the face mesh elements. The face mesh therefore can be modified without changing the geometry of the muscle structure. Similarly, the muscle anatomy or other embedded structures can be manipulated without affecting the face geometry. This can be especially useful when adding new structures to the face model, such as missing muscles or aponeurosis and tendon complexes.

Previous studies into numerical modelling of muscle contractions have also demonstrated the importance of 3-D geometry in generating non-uniform strain distribution observed in experiments [24]. Since the force generated by a muscle fibre varies as a function of its stretch, the non-uniform strain of muscle fibres must be accommodated when evaluating their active and passive stresses at various activation levels. In addition to obtaining non-uniform strain along fascicles, a 3-D model is also able to predict the change of the PCSA of fascicles during deformation, thus improving the predictability when tissues undergo large straining.

In formulating the muscle models, a continuous locally varying finite element field of Euler angles is used to describe fibre pennations in pennate and convergent muscles. Although not included in this paper, a further advantage of using piecewise polynomial representation is that parameters that define these angles (at element nodes) can be efficiently fitted to anatomical measurements using linear least square methods. The challenge is to obtain anatomical fibre orientations *in vivo*, one possibility is to use diffusion tensor magnetic resonance imaging (DT-MRI) and studies on reconstructing myocardial fibres using DT-MRI have already shown some promising results [32]. In addition to fibre angles, activations levels can also be interpolated using piecewise polynomials. This allows us to investigate spatially varying activation patterns and make effective use of measurements such as facial surface electromyography [33].

In summary, representation of 3-D muscle geometry is vital when an accurate and reliable mechanical simulation of the facial expression is desired. Despite this, there have not been many face models with 3-D muscle structures. This is primarily due to the complexity of facial musculatures, which can significantly increase the computational cost of an already expensive problem. We have solved this problem by

evaluating 3-D muscle structures as an array of discrete point loads that are defined at the integration points of an appropriate quadrature scheme. The method introduced here offers the potential to enhance the accuracy of models of the face without adding too much computational cost. One limitation of our method is that since the whole model is assumed to be in a single continuum, the interaction between muscles and surrounding tissues, and between separate muscle structures cannot be studied. One of our future works is to extend this method, to allow sliding and contact interactions between internal structures, by using the extended finite-element method to decouple the stresses and strains across the muscle boundary.

Acknowledgement

The work presented in this paper was funded by Foundation for Research, Science and Technology of New Zealand under the grant number UOAX0712.

References

[1] E. Sifakis, I. Neverov, R. Fedkiw, Automatic determination of facial muscle activations from sparse motion capture marker data, ACM T Graphic, 24 (2005) 417-425.

[2] L. Ramirez-Valdez, R. Hasimoto-Beltran, 3D-Facial Expression Synthesis and its Application to Face Recognition Systems, J Appl Res Technol, 7 (2009) 323-339.

[3] M. Bucki, M.A. Nazari, Y. Payan, Finite element speaker-specific face model generation for the study of speech production, Comput Methods Biomech Biomed Engin, 13 (2010) 459-467.

[4] L. Beldie, B. Walker, Y. Lu, S. Richmond, J. Middleton, Finite element modelling of maxillofacial surgery and facial expressions - a preliminary study, Int J Med Robot Comp, 6 (2010) 422-430.

[5] H. Kim, P. Jurgens, L.P. Nolte, M. Reyes, Anatomically-driven soft-tissue simulation strategy for cranio-maxillofacial surgery using facial muscle template model, Med Image Comput Comput Assist Interv, 13 (2010) 61-68.

[6] V. Macchi, C. Tiengo, A. Porzionato, C. Stecco, E. Vigato, A. Parenti, B. Azzena, A. Weiglein, F. Mazzoleni, R. De Caro, Histotopographic study of the fibroadipose connective cheek system, Cells Tissues Organs, 191 (2010) 47-56.

[7] B. Mendelson, Facelift anatomy, SMAS, retaining ligaments and facial spaces, in: S.J. Aston, D.S. Steinbrech, J. Walden (Eds.) Aesthetic Plastic Surgery, Saunders, Edinburgh, 2009, pp. 6:1-22.

[8] Y.C. Fung, Biomechanics : mechanical properties of living tissues, 2nd ed., New York: Springer-Verlag, 1993.

[9] K. Waters, A muscle model for animation three-dimensional facial expression, Comput Graphics, 21 (1987) 17-24.

[10] R.M. Koch, M.H. Gross, A.A. Bosshard, Emotion editing using finite elements, Comput Graph Forum, 17 (1998) 295-302.

[11] Y. Zhang, E.C. Prakash, E. Sung, Face alive, J Visual Lang Comput, 15 (2004) 125-160.

[12] E. Gladilin, S. Zachow, P. Deuflhard, H.C. Hege, Anatomy- and physics-based facial animation for craniofacial surgery simulations, Med Biol Eng Comput, 42 (2004) 167-170.

[13] M.A. Nazari, P. Perrier, M. Chabanas, Y. Payan, Simulation of dynamic orofacial movements using a constitutive law varying with muscle activation, Comput Method Biomec, 13 (2010) 469-482.

[14] M. Chabanas, V. Luboz, Y. Payan, Patient specific finite element model of the face soft tissues for computer-assisted maxillofacial surgery, Med Image Anal, 7 (2003) 131-151.

[15] V. Spitzer, M.J. Ackerman, A.L. Scherzinger, D. Whitlock, The visible human male: a technical report, J Am Med Inform Assoc, 3 (1996) 118-130.

[16] J.T. Oden, Finite elements of nonlinear continua, New York: McGraw-Hill, 1972.

[17] O.C. Zienkiewicz, R.L. Taylor, J.Z. Zhu, The finite element method : its basis and fundamentals, 6th ed., Amsterdam ; London: Elsevier Butterworth-Heinemann, 2005.

[18] C.P. Bradley, A.J. Pullan, P.J. Hunter, Geometric modeling of the human torso using cubic hermite elements, Ann Biomed Eng, 25 (1997) 96-111.

[19] G.G. Barbarino, M. Jabareen, E. Mazza, Experimental and numerical study of the relaxation behavior of facial soft tissue, Proc Appl Math Mech, 9 (2009) 87-90.

[20] P.J. Flory, Thermodynamic relations for high elastic materials, T Faraday Soc, 57 (1961) 829-838.

[21] A.F. Huxley, Muscle structure and theories of contraction, Prog Biophys Biophys Chem, 7 (1957) 255-318.

[22] A.F. Huxley, R.M. Simmons, Proposed mechanism of force generation in striated muscle, Nature, 233 (1971) 533-538.

[23] F.E. Zajac, Muscle and tendon: properties, models, scaling, and application to biomechanics and motor control, Crit Rev Biomed Eng, 17 (1989) 359-411.

[24] S.S. Blemker, P.M. Pinsky, S.L. Delp, A 3D model of muscle reveals the causes of nonuniform strains in the biceps brachii, J Biomech, 38 (2005) 657-665.

[25] S. Standring, Gray's anatomy : the anatomical basis of clinical practice, in, Edinburgh: Churchill Livingstone, (2008), pp. xxiv, 1551 p.

[26] K. Mithraratne, A. Hung, M. Sagar, P.J. Hunter, An Efficient Heterogeneous Continuum Model to Simulate Active Contraction of Facial Soft Tissue Structures, in: C.T. Lim, J.C.H. Goh (Eds.) IFMBE Proceedings: 6th World Congress of Biomechanics; August 1-6, 2010; Singapore, Springer Berlin Heidelberg, 2010, pp. 1024-1027.

[27] L.M. Dzubow, The fasciae of the face: an anatomic and histologic analysis, J Am Acad Dermatol, 14 (1986) 502-507.

[28] T. Wu, K. Mithraratne, M. Sagar, P.J. Hunter, Characterizing Facial Tissue Sliding Using Ultrasonography, in: C.T. Lim, J.C.H. Goh (Eds.) IFMBE Proceedings: 6th World Congress of Biomechanics; August 1-6, 2010; Singapore, Springer Berlin Heidelberg, 2010, pp. 1566-1569.

[29] J.W. Fernandez, P. Mithraratne, S.F. Thrupp, M.H. Tawhai, P.J. Hunter, Anatomically based geometric modelling of the musculo-skeletal system and other organs, Biomech Model Mechanobiol, 2 (2004) 139-155.

[30] R. Ozdemir, H. Kilinc, R.E. Unlu, A.C. Uysal, O. Sensoz, C.N. Baran, Anatomicohistologic study of the retaining ligaments of the face and use in face lift: Retaining ligament correction and SMAS plication, Plast Reconstr Surg, 110 (2002) 1134-1147.

[31] S.S. Blemker, S.L. Delp, Three-dimensional representation of complex muscle architectures and geometries, Ann Biomed Eng, 33 (2005) 661-673.

[32] L. Zhukov, A.H. Barr, Heart-muscle fiber reconstruction from diffusion tensor MRI, IEEE Visualization 2003, Proceedings, (2003) 597-602.

[33] N.P. Schumann, K. Bongers, O. Guntinas-Lichius, H.C. Scholle, Facial muscle activation patterns in healthy male humans: a multi-channel surface EMG study, J Neurosci Methods, 187 (2010) 120-128.

Published in Finite Elements in Analysis and Design, 76: pp. 63-70.
DOI: 10.1016/j.finel.2013.08.002

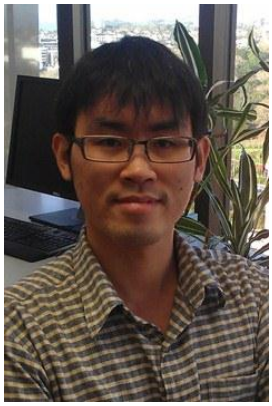

Tim Wu is a doctoral student studying at Auckland Bioengineering Institute (The University of Auckland, New Zealand). He completed his BE(1st Hons) at The University of Auckland, specialised in Biomedical Engineering in 2008. Tim's doctoral thesis is focused on the contact and sliding interaction between various soft-tissue structures underneath the facial skin. His goal is to improve the accuracy and reliability of existing finite element models of the face for applications in the medical field.

Alice Pui-Lam Hung is a doctoral student studying at Auckland Bioengineering Institute (The University of Auckland, New Zealand). She received a Bachelor of Engineering in Software Engineering (1st Hon) from the same University. Her primary research focus is to gain an in-depth understanding of facial soft tissue mechanics with the objective of constructing a 3D biomechanical model for simulating facial expressions. Her goal is to develop facial modelling techniques and make use of anatomically accurate descriptions through reconstruction from medical images of facial structures to achieve physically realistic results.

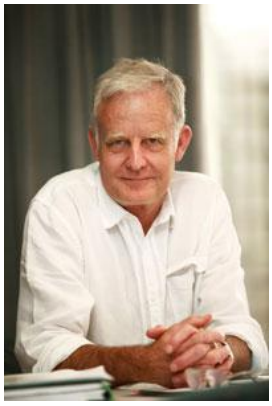

Peter Hunter completed his BE and ME degrees at The University of Auckland before undertaking his DPhil in Physiology at the University of Oxford, researching finite element modeling of ventricular mechanics. As Co-Chair of the Physiome Committee of the IUPS, Peter is helping to develop modelling infrastructure for the use of computational methods for understanding the integrated physiological function of the body in terms of the structure and function of tissues, cells and proteins. Alongside his role as Director of the Auckland Bioengineering Institute at The University of Auckland, Peter is also Director of Computational Physiology at Oxford University.

Published in Finite Elements in Analysis and Design, 76: pp. 63-70.
DOI: 10.1016/j.finel.2013.08.002

Kumar Mithraratne is a Senior Research Fellow and Principal Investigator in the Auckland Bioengineering Institute at the University of Auckland. He holds a PhD in Mechanical Engineering from the National University of Singapore, an MSc degree with Distinction in Mechanical Engineering from King's College London, University of London and a BScEng degree in Chemical Engineering from the University of Moratuwa, Sri Lanka. His research interests include musculoskeletal system modelling, soft tissue computational mechanics, flow mechanics, finite element analysis and gait analysis.